Nexus Network Journal (2025) 27:639–661
https://doi.org/10.1007/s00004-025-00816-0

NEXUS NETWORK JOURNAL
Architecture and Mathematics

RESEARCH

Estimating the Minimum Thickness of Earthquake-Resistant Vaults and Catenary Arches by Using a Hanging Chain

Rodrigo Martín-Sáiz[1] · **Blas Herrera**[2]

Accepted: 12 March 2025 / Published online: 14 April 2025

Abstract

This paper presents a procedure for estimating the minimum thickness of vaults and catenary arches to resist seismic in-plane horizontal loading. In order to define the shapes of the thrust lines that result from combining the self-weight of the arches and horizontal in-plane acceleration, an inverted hanging chain was used. The chain inclines the line by connecting its ends horizontally. Subsequently, iterative calculation help find the minimum thickness of the catenary arches with constant section that inscribe the defined thrust lines. This procedure was applied to different arches by considering ten values of horizontal acceleration. Consequently, graphs were drawn that relate the horizontal acceleration to the minimum thickness, contingent on the rise/span ratio of each arch, as well as the position of the hinges created in the collapse mechanism. Finally, the application is shown through the intersections of several catenary arches.

Keywords Vaults and catenary arches · Thrust line · Minimum thickness · Hanging chain · Seismic loads

Introduction

The principle of using an inverted hanging chain to define the ideal shape of an arch or vault under self-weight loads (Hooke 1676) is a well-established concept which has been widely used since the eighteenth century (Graefe 2020). The Catalan modernist architect Antoni Gaudí took the literal interpretation of this principle to an extreme. Gaudí used hanging models made of ropes and small sandbags to define arches and vaults with highly intricate shapes, as evidenced by his work on the Sagrada Familia temple in Barcelona and the crypt of the

✉ Rodrigo Martín-Sáiz
rodrigo.martin@urv.cat

[1] School of Architecture, Universidad Rovira I Virgili, Av. de La Universitat, 43204 Reus, Spain

[2] Department of Computing Engineering and Mathematics, Universitat Rovira I Virgili, Av. Paisos Catalans 26, 40307 Tarragona, Spain

Colonia Güell (Huerta 2006). More than half a century later, the Swiss engineer Heinz Isler designed complex shell structures by inverting the shape obtained in models built with hanging nets (Boller et al. 2024). The shape obtained in models built with chains, ropes or hanging nets is independent of the scale and magnitude of the loads, but rather depends on the manner in which these loads are distributed along the hanging elements (Addis 2014). Currently, the use of hanging chain physical models remains a simple and precise method for obtaining funicular shapes such as those that describe the thrust lines of arches and vaults (Sunguroglu and Baraut 2013; Miccoli et al. 2023; Afonso and Fialho 2024; Borhani and Kalanta 2024; Fallacara et al. 2024).

The catenary is the curved shape that a chain of uniform weight assumes when suspended between two fixed points. The equation was formulated several years after the discovery of the principle of the inverted hanging chain (Bernoulli 1691; Huygens 1691; Leibniz 1691; Gregory 1697). Subsequently, the catenary has been regarded as the best form of an arch of constant section when the sole load acting is its self-weight. In a manner analogous to the simple tensioning of a chain as a result of inversion, the catenary arch should be simply compressed, without bending moments. The subject of catenary arches remains a focus of research, with the objective of developing new methods of structural analysis and design (Gohnert and Bradley 2020; Li, et al. 2024; Wang and Zhang 2024).

In recent years, several studies have demonstrated that there is no exact coincidence between the geometric axis and the centroildal axis of a catenary arch with constant rectangular cross-section (Tempesta and Galassi 2019; Nikolić 2019 and 2022; Nodargi and Bisegna 2020; Alexakis and Makris 2023). The geometric axis is defined by the catenary curve that joins the centroids of all its cross-sections. The centroidal axis is defined by the line joining the centres of gravity of all the infinitesimal voussoirs which make up the arch considering a normal stereotomy. This discrepancy between the two axes precludes the possibility of the arch being free of bending moments. However, as the discrepancy is minimal, it has no practical consequence from a mechanical point of view. In other words, notwithstanding the above, the catenary method remains the most efficient approach for constructing a constant-section arch. This is the assumption that has been made in this study.

The question of the minimum thickness of an arch required to resist gravity loads has been a topic of considerable interest throughout the history of construction (Heyman 1969; Huerta 2019). The issue remains a topic of ongoing research in the mechanics of circular arches (Makris and Alexakis 2013; Forgács et al. 2017), pointed arches (Nikolić 2017; Lengyel 2018) and elliptical arches (Alexakis and Makris 2013). The optimal design of vaults and arches subjected to in-plane horizontal seismic loading has also been a recurring research topic in recent years. This has included the development of envelope shapes for the thrust lines resulting from gravity loads and seismic horizontal accelerations in both directions (Michiels and Adriaenssens 2018; Málaga-Chuquitaype et al. 2022; Kalapodis et al. 2022 and 2023). In addition, the minimum constant thickness needed to inscribe these thrust lines has been calculated (Alexakis and Makris 2014 and 2023; Cavalagli et al. 2016; Ricci et al. 2019; Kampas et al. 2021; McLean et al. 2021; Ther and Kollár 2021).

In all these instances, the issue has been addressed exclusively through analytical means, namely through the formulation of mathematical models.

The use of vaults and catenary arches became more relevant in the last years, attending to the environmental problem (De Wolf et al. 2016), especially in developing countries (Granier et al. 2006, Block et al. 2010, Ramage et al. 2010, Bradley et al. 2017 and 2018, Gohnert et al. 2018). This is because it is possible to build easily these elements, vaults and arches, using local labor and local materials. These materials have often low resistance properties, like stone masonry, bricks or even earth bocks (Dahmen and Ochsendorfs 2012). The use of earth blocks in the construction is extended in many zones around the world, especially in Africa, Southeast of Asia and South America (Vyncke et al. 2018). Some of these zones have a moderate or high seismic hazard. Some of these zones have defined moderate or high seismic accelerations. This issue can be consulted on the global seismic hazard map of the Global Earthquake Model (Johnson et al. 2023).

This paper presents a straightforward procedure for estimating the minimum thickness of vaults and catenary arches of constant section capable of resisting in-plane horizontal loading due to an earthquake. The procedure is founded upon Hooke's Chain Theory. This procedure is intended to be easy to use. Thus, its use will not be conditioned by access limitations to specific software. For this reason, we have minimized the use of numerical methods which have been described for easy application by architects and engineers. This issue is especially relevant for developing countries.

The use of hanging chain models could present two difficulties: the equivalence of the load distribution of the chain model and the real model, and the capture of the funicular shape obtained. Nevertheless, these difficulties are minimal in the presented method. Firstly, because the load is uniformly distributed in a catenary arch and, for this reason, only a chain of uniform weight is required. Secondly, because, in this case, the hanging chain model used is two-dimensional and the capture of the funicular shape obtained can be done through a simple photograph.

Method

Outline of the Procedure

The procedure is comprised of two parts. The first part involves the use of hanging chain models. By tilting the straight line containing the ends of the chain with respect to the horizontal, different combinations of seismic and gravitational accelerations result in different thrust lines of a catenary arch. In the second part of the procedure, an iterative calculation is then performed to determine the minimum thickness of the constant-section catenary arch which inscribes the three thrust lines (the line resulting from its self-weight and the two lines resulting from the combination of its self-weight with the horizontal seismic acceleration in both directions).

This procedure considers the minimum thickness of the arch for inscribing the thrust lines due to a horizontal seismic acceleration, but not the material resistance, the effects due to other load cases such as wind, snow or other live loads, or the

buckling due an excessive slenderness. These issues must be assessed thought other procedures.

Thrust Lines of a Catenary Arch Subjected to Horizontal Acceleration

In a graphic statics analysis of an arch subjected to horizontal acceleration, it is common to tilt the analysed object by an angle α whose tangent is equal to the ratio λ between the horizontal seismic acceleration a and gravity's force g (Eq. 1). Ratio λ expresses a portion of g acting in the horizontal direction (Block et al. 2006; DeJong 2009; Alexakis and Makris 2023). Therefore, in addition to the vertical loads due to the self-weight of the arch, we consider equivalent static forces in the horizontal direction. These forces are obtained by multiplying the mass of the arch at each point by the seismic acceleration (Heyman 1966 and 1969).

$$\lambda = \tan \alpha = \frac{a}{g} \tag{1}$$

The tilting of the horizontal plane was used with block models to determine the collapse shapes of an arch subjected to the action of its self-weight combined with a horizontal acceleration (Misseri et al. 2018). We used the same device (i.e. tilting the analysed object) to obtain the thrust lines of a catenary arch subjected to horizontal seismic acceleration. Next, a rigid rectangular panel 70×50 cm was taken, and placed it in a vertical plane with a suspended chain composed of spheres ø 3.5 mm. As a result, the ends were anchored at a fixed distance $s = 60$ cm along one of the edges. When this edge coincides with the horizontal direction, the chain takes the form of a catenary whose axis of symmetry is vertical (Fig. 1a). It is known that this inverted catenary coincides with the thrust line of a one-dimensional arch with evenly distributed weight. If the edge of the plate is tilted by an angle α, the original catenary is deformed and loses its symmetry (Fig. 1b). This new shape, rotated again by an angle—α and inverted, coincides with the line of thrust of a one-dimensional arch subjected to its self-weight and also to a horizontal acceleration a such that $a = \lambda g$, where λ is a function of the angle α according to Eq. (1) (Fig. 1c). The panel was marked with an indicator of α angles, which are identified by the value of their tangent, i.e., the value of λ. We hung another chain from one of its ends at the centre of the upper edge of the panel, so that when the edge of the panel is tilted by an angle α, this chain indicates the corresponding value of λ. The accuracy of the angle measurement depends on the instrument used. This means that the angle can be measured with the naked eye or with a laser meter. As explained below, this affects the accuracy of the results obtained by this method, especially for arches with small *r/s* ratios and small horizontal accelerations.

For reproducing and using the found shapes, photographs were taken and converted into a CAD drawing. In this process, we can use specific image vectorization software or simply redraw the referenced photograph using CAD software. Alternatively, we can use photogrammetry technique (Afonso and Fialho 2024) or laser scanning. In any case, we obtain a cloud of points corresponding

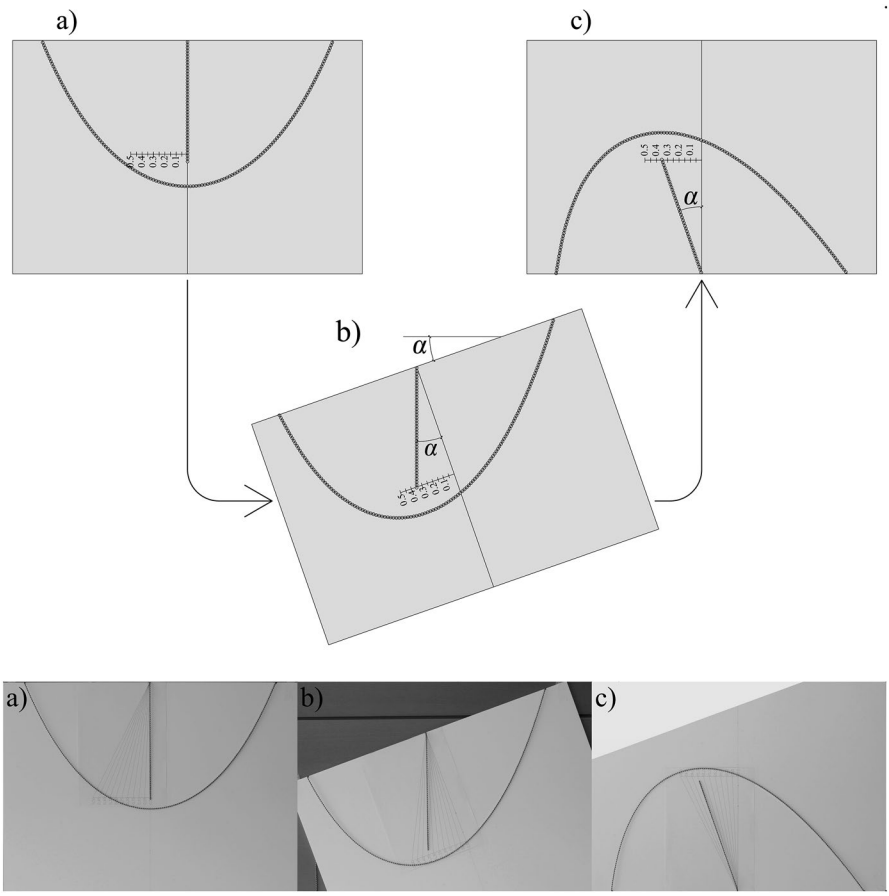

Fig. 1 Obtaining the thrust line of a one-dimensional catenary arch subjected to the combined action of gravity and a horizontal acceleration: drawings of the process and photographs of the physical model

to each line of thrust. The means used to reproduce and convert the shape into a point cloud, as well as the number of points defining each thrust line, determine the accuracy of the results obtained. Taking into account the simplicity of this two-dimensional physical model, photographing and redrawing in CAD may be sufficient for an accurate capture of the shape found. This avoids procedure limitations due to use constraints of specific software.

Then, in order to present some examples of application, this study considered three arches whose ratios *r/s* are 0.33, 0.50 and 0.67; where *r* is the maximum rise of the arch and *s* is the span. Following the procedure, we have obtained the thrust line of each of the three arches, considering ten horizontal accelerations between $a = 0.05$g and $a = 0.50$g (Figs. 2, 3 and 4). This range of seismic accelerations is not representative of any specific geographic area, but it is possible to associate these values with those defined for the seismic zones in the North and the East

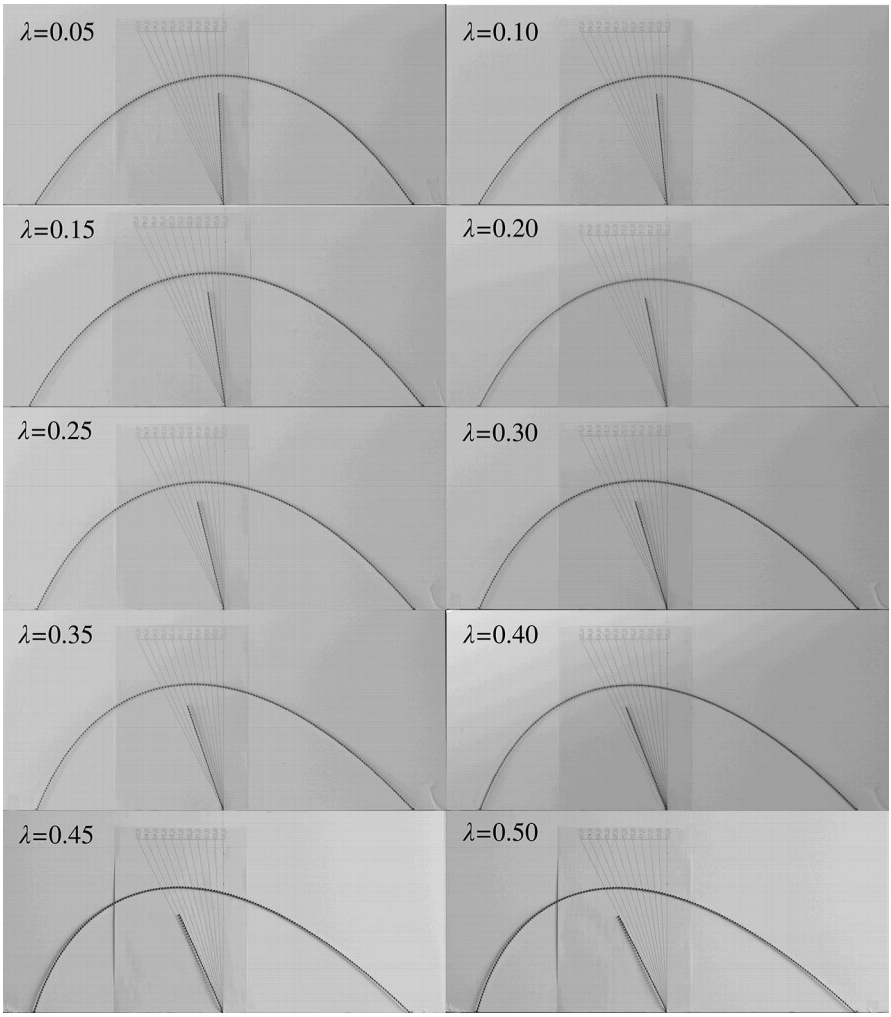

Fig. 2 Thrust lines of a catenary arch with $r/s = 0.33$, considering ten horizontal accelerations between $a = \lambda g$ with $\lambda = 0.05 \div 0.50$ by using a hanging chain

of the African continent (Johnson et al. 2023). In any case, other higher values of horizontal accelerations can be considered in this method.

Calculation of the Minimum Arch Thickness

The shape of the catenary is defined by Eq. (2). If we consider a catenary arch with rise r and span s, with its ends situated on the x-coordinate axis and with its highest point on the y-coordinate axis, we can ascertain the values of the parameters b and c by substituting the points $(-s/2, 0)$, $(0, r)$ and $(s/2, 0)$, expressed in Cartesian coordinates

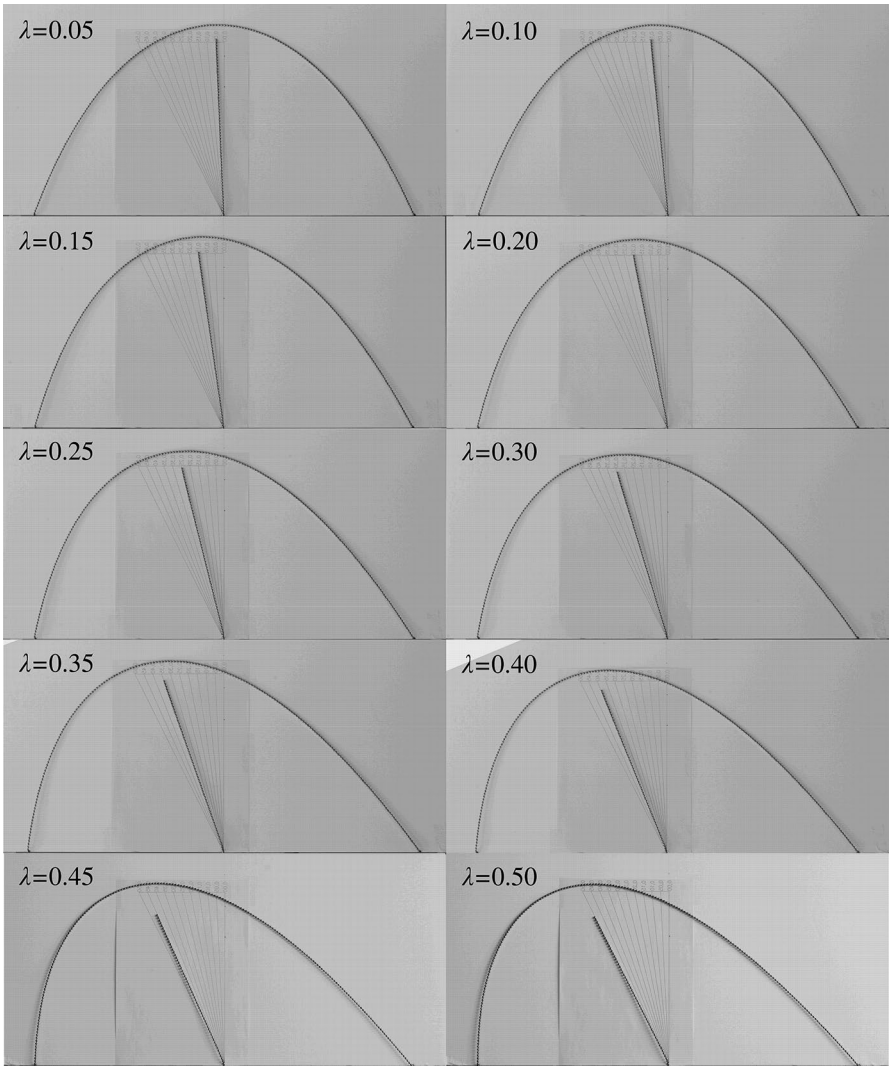

Fig. 3 Thrust lines of a catenary arch with $r/s = 0.50$, considering ten horizontal accelerations between $a = \lambda g$ with $\lambda = 0.05 \div 0.50$ by using a hanging chain

(x, y), in Eq. (2). Thus, we find that $c = r - b$ and that b can be derived from Eq. (3). To determine the value of b, the well-known Newton–Raphson iterative method can be employed.

$$y = b \cosh\left(\frac{x}{b}\right) + c \tag{2}$$

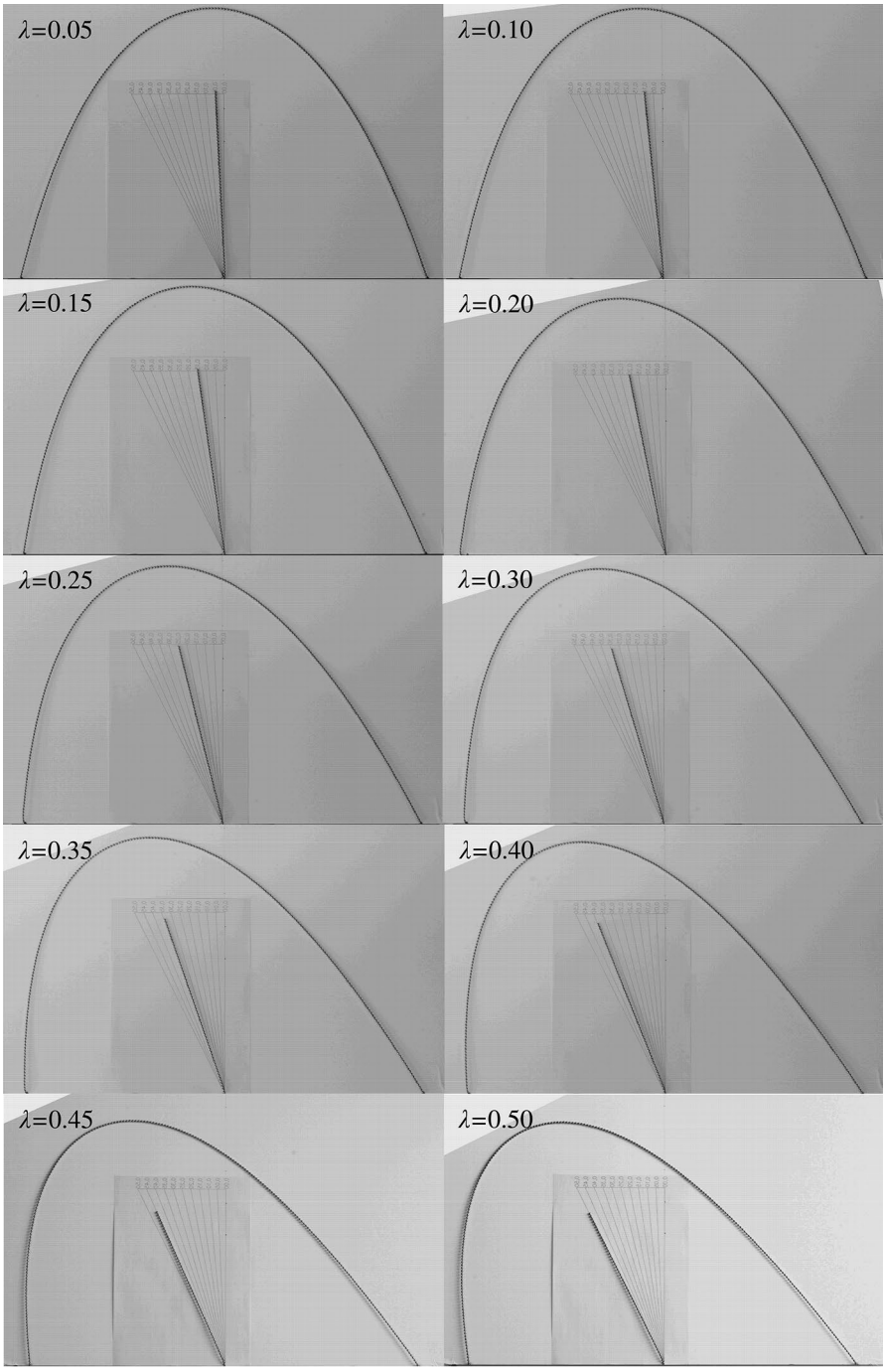

Fig. 4 Thrust lines of a catenary arch with $r/s = 0.67$, considering ten horizontal accelerations between $a = \lambda g$ with $\lambda = 0.05 \div 0.50$ by using a hanging chain

$$b\cosh\left(\frac{s}{2b}\right)+r-b=0 \tag{3}$$

Figure 5 shows the variation of the ratio *b/s* of the catenary curve as a function of the arch's *r/s* ratio obtained by means of the procedure described in the previous paragraph. This graphic provides an easy way to calculate the parameters of the catenary curves for vaults and arches with $0.1 \leq r/s \leq 2.0$.

Therefore, on one hand, we have the thrust line resulting from the arch's self-weight. The catenary shape of this thrust line is defined by the parameters *b* and *c* in Eq. (2). On the other, we have the point cloud of the thrust line which has been found for a given horizontal acceleration *a*, and the point cloud of its symmetric thrust line. These three curves are designated as thrust line 1, thrust line 2, and thrust line 3, respectively (Fig. 6a). The three lines converge at points *A* and *B*. To achieve mechanical feasibility, it is necessary that all three thrust lines are inscribed within the arch. Subsequently, the minimum thickness t_{min} that the arch must have to withstand a given horizontal seismic acceleration is defined as twice the smallest possible distance between the catenary (thrust line 1) and the furthest point of the thrust line found for a given horizontal acceleration and its symmetric (thrust lines 2 and 3). To minimise the aforementioned distance, thrust lines 2 and 3 are shifted from points *A* and *B* to points *A'* and *B'*, i.e. they are shifted a distance *d* in the horizontal direction and a distance *e* in the vertical direction until t_{min} is found (Fig. 6b). The method of shifting the thrust line resulting from the horizontal acceleration has previously been employed in the assessment and

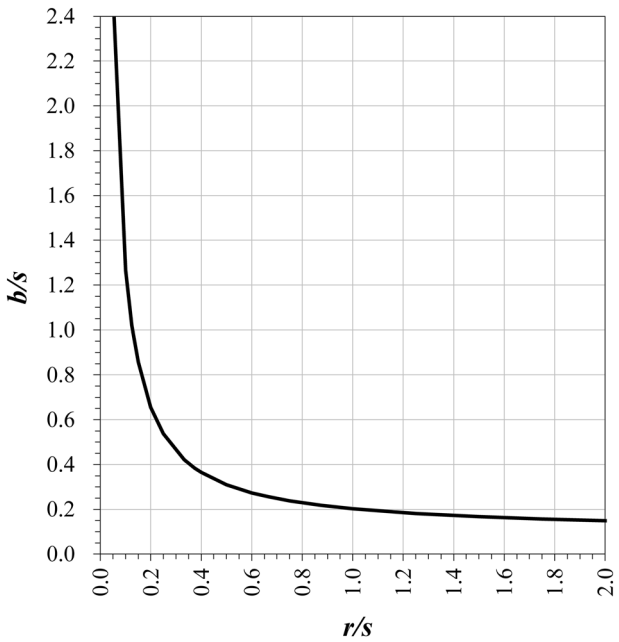

Fig. 5 Variation of the ratio *b/s* of the catenary curve as a function of the arch's ratio *r/s*

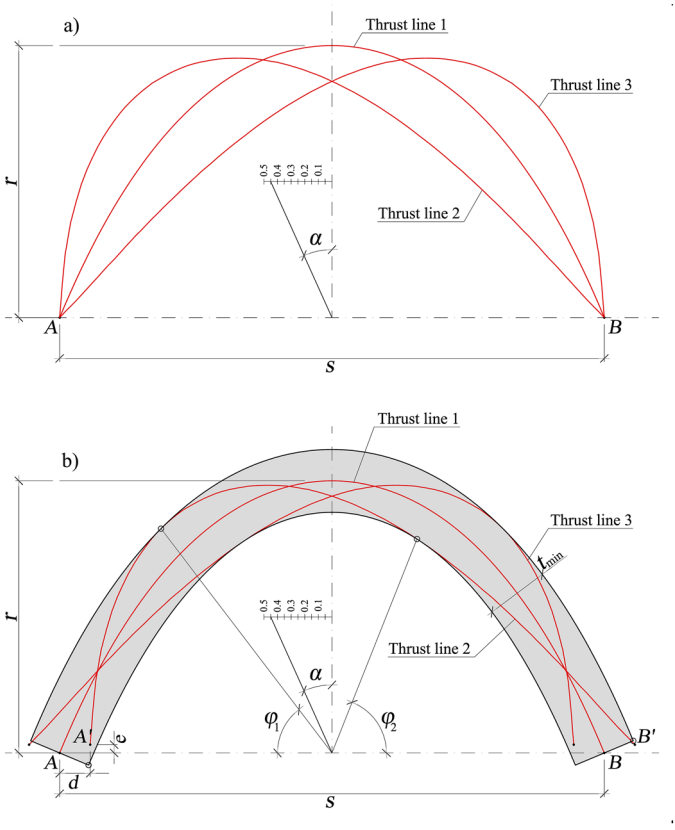

Fig. 6 **a** Three thrust lines of the catenary arch, resulting from the arch's self-weight and from the horizontal acceleration $a = 0.45g$ in both directions. **b** Catenary arch of minimum thickness inscribing the three thrust lines

design of earthquake-resistant arches, but not with the aim of minimising their thickness, but with the aim of minimising the amount of material used in variable thickness arches (Michiels and Adriaenssens 2018). Figure 3b illustrates that, in an arch with $t_{\min}$, the thrust lines resulting from the horizontal acceleration intersect the arch contour at four points, mirroring the formation of the four hinges characteristic of the arch collapse mechanism (Alexakis and Makris 2014 and 2023; Cavalagli et al. 2016; Kampas et al. 2021; McLean et al. 2021; Ther and Kollár 2021). Two of the hinges are located at the base of the arch, while the other two are located at two intermediate points, as defined by the angles φ_1 and φ_2.

The mathematical process for determining $t_{\min}$ is outlined below: For each given point p, with coordinates (x_p, y_p), in the point cloud making up thrust line 2, the distance d_p from the points on thrust line 1 is defined in the Eq. (4). Then, to find the minimum value of d_p, we use numerical programming and the Newton–Raphson method to calculate the zero of the derivative of the function

$d_p(x)$ in Eq. (5). That is, we calculate the zero θ_p of Eq. (5). Then, we calculate the minimum distance $d_{p,\min}$ with Eq. (6).

$$d_p = \sqrt{\left(x_p - x\right)^2 + \left(y_p - b\sinh\left(\frac{x}{b}\right) - c\right)^2} \tag{4}$$

$$2x - 2x_p - 2y_p \sinh\left(\frac{x}{b}\right) + b\sinh\left(\frac{2x}{b}\right) + 2c\sinh\left(\frac{x}{b}\right) = 0 \tag{5}$$

$$d_{p,\min} = \sqrt{\left(x_p - \theta_p\right)^2 + \left(y_p - b\sinh\left(\frac{\theta_p}{b}\right) - c\right)^2} \tag{6}$$

Alternatively, for a given point p, in the cloud of points making up thrust line 2, we calculate the distance $d_{p,i}$ using Eq. (7) for all points $q_i = \left(x_i, y_i\right)$ in the cloud of points making up thrust line 1, i.e., points on the catenary; and $d_p = \min\left(d_{p,i}\right)$ the minimum of all $d_{p,i}$. This second way does not need numerical iterative methods to find the solution.

$$d_{p,\min} = \sqrt{\left(x_p - x_i\right)^2 + \left(y_p - y_i\right)^2} \tag{7}$$

In any case, if this calculation is carried out for all points of thrust line 2, the minimum value of thickness t for thrust line 2 is found, which is the double of $\max\left(d_{p,\min}\right)$ the maximum of all $d_{p,\min}$. Similarly, the minimum value of thickness t for thrust line 3 is obtained by symmetry. The same calculation is then numerically iterated with discrete shifts d and e of the thrust lines (Fig. 6b), with numerical increments of ten thousandths of a unit in both the horizontal and vertical directions. Once the minimum value has been calculated as a function of d and e, the final value of thickness, $t_{\min}$, is obtained. For computational purposes, the maximum value of horizontal shift, d, is defined as the distance from vertex A to the origin of coordinates, while the maximum value of vertical shift, e, is defined as the distance from the point where thrust line 1 intersects the Y axis to the point where thrust line 2 intersects the Y axis.

Subsequently, the minimum thickness $t_{\min}$ was calculated for the thirty cases shown in Figs. 2, 3 and 4, considering three different arches and ten horizontal accelerations between $a = 0.05g$ and $a = 0.50g$. In all cases, a total of 101 points were used to define each thrust line. Figures 7, 8 and 9 illustrate the thirty resulting arches in the same sequence as in Figs. 2, 3 and 4, with the three thrust lines of each arch delineated by a red line.

Note that the thrust lines of the arches with $\lambda = 0.05$ and $\lambda = 0.10$ in Fig. 7 are almost indistinguishable from the arch itself. The same happens in the arch in the arch with $\lambda = 0.05$ in Fig. 8. There is a relationship between the slenderness of the resulting arch and the accuracy of the method, as discussed below.

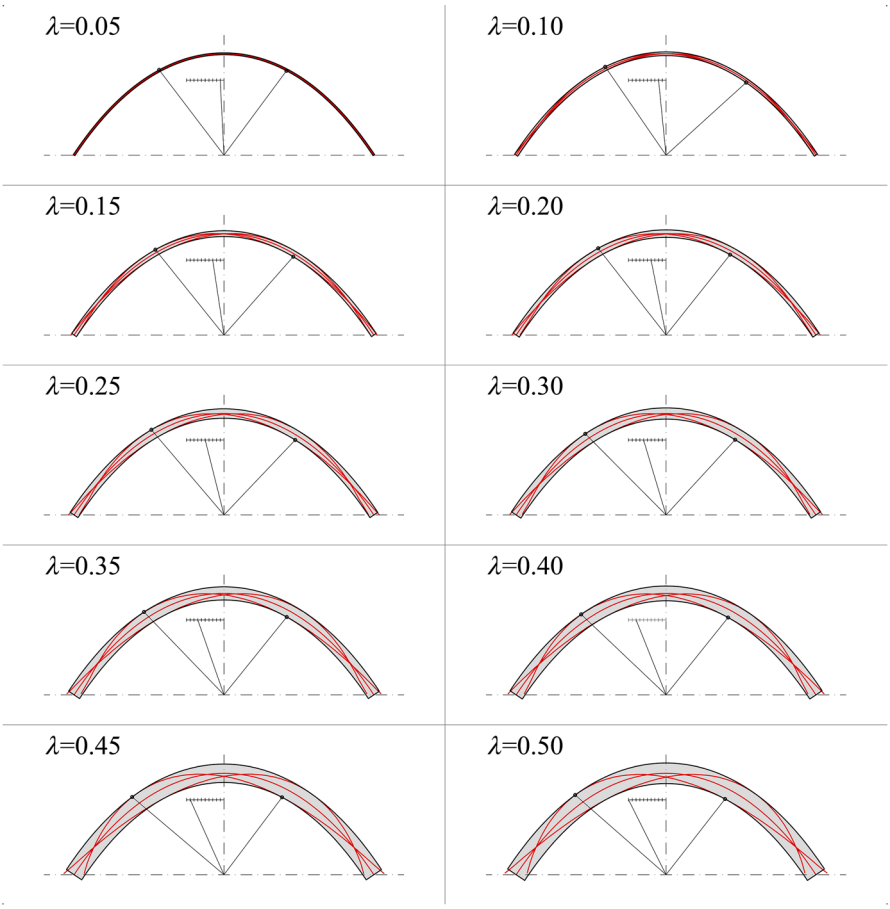

Fig. 7 Minimum thickness $t_{\min}$ of catenary arches with $r/s = 0.33$ considering ten horizontal accelerations $a = \lambda g$ with $\lambda = 0.05 \div 0.50$. The resulting thrust lines are defined in red (Colour figure online)

Analysis of the Results

The results obtained in the aforementioned examples were subjected to analysis and presented in three graphs. In the first graph (Fig. 10), the horizontal axis represents the horizontal acceleration (a) as a multiple of the gravitational acceleration (g), and the vertical axis represents the ratio t_{min}/s. Therefore, each of the three curves displayed in this graph represents the variation in the minimum thickness of an arch as a function of the horizontal seismic acceleration it must resist, considering arches with three different r/s ratios. The shape of these three curves is very similar to that of three straight lines passing through the origin of coordinates. The equation of these three straight lines was defined using the well-known method of least squares. Thus, for catenary arches with $r/s = 0.33$, we found that $t_{\min}/s = 0.130a$; for arches with $r/s = 0.50$, we found that $t_{\min}/s = 0.254a$, and for arches with $r/s = 0.67$, we

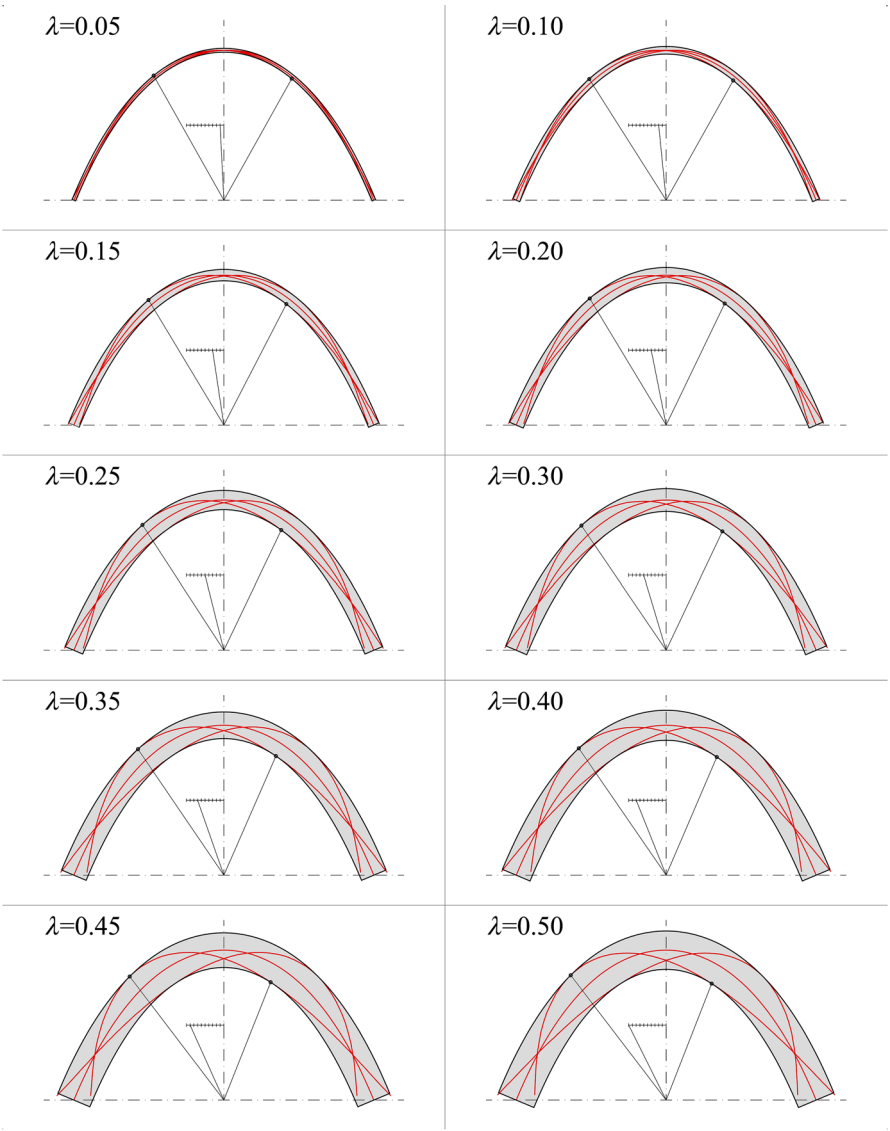

Fig. 8 Minimum thickness t_{min} of catenary arches with $r/s = 0.50$ considering ten horizontal accelerations $a = \lambda g$ with $\lambda = 0.05 \div 0.50$. The resulting thrust lines are defined in red (Colour figure online)

found that $t_{min}/s = 0.385a$. It should be noted that the aforementioned equations are only valid for values of $a \in [0.05g, 0.50g]$.

In the second graph (Fig. 11), the horizontal axis represents the r/s ratio of the catenary arch, and the vertical axis represents the ratio t_{min}/s required to resist ten different horizontal accelerations. Once more, the shape of each of the ten curves represented in this graph is similar to that of a straight line. As the aforementioned

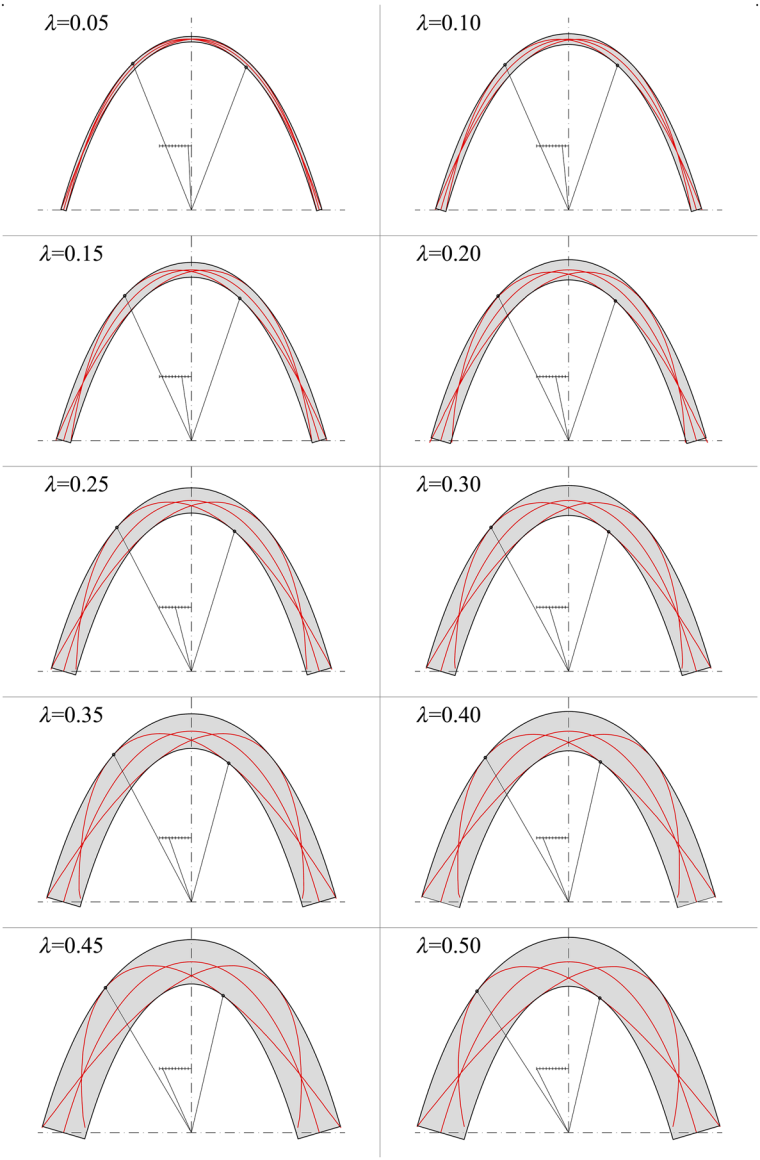

Fig. 9 Minimum thickness t_{min} of catenary arches with $r/s = 0.67$ considering ten horizontal accelerations $a = \lambda g$ with $\lambda = 0.05 \div 0.50$. The resulting thrust lines are defined in red (Colour figure online)

straight lines do not pass through the origin of coordinates, we defined their equation $t_{min}/s = mr/s + n$ by means of regression analysis. Table 1 presents the parameters m and n for each line. It should be noted that the equations presented herein are only valid for catenary arches with $r/s \in [0.33, 0.67]$.

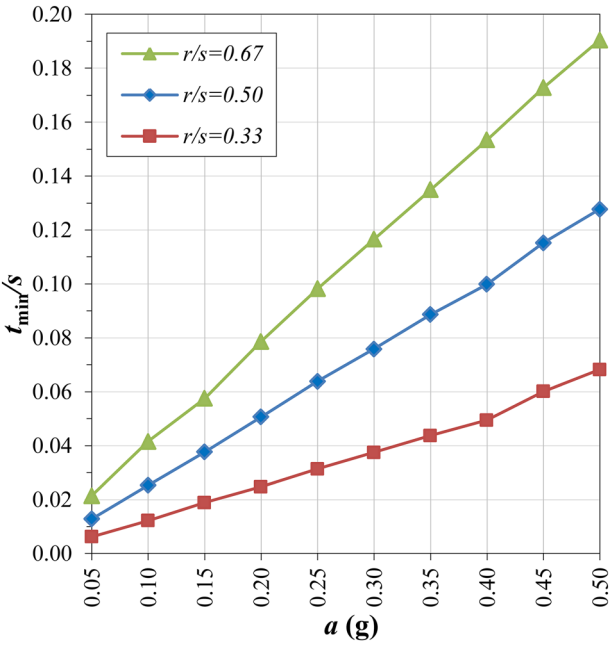

Fig. 10 Relationship between seismic acceleration and the minimum thickness t_{min} of a catenary arch, considering three different *r/s* ratios

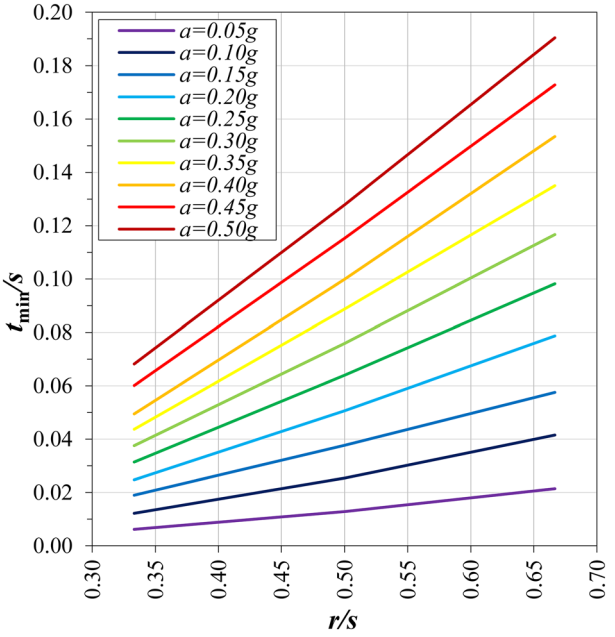

Fig. 11 Relationship between the shape of the catenary arch, as defined by the ratio *r/s*, and the minimum thickness t_{min} to resist ten horizontal accelerations between $a = 0.05g$ and $a = 0.50g$

Table 1 Parameters m and n of the equations for the straight lines which relate t_{min} to the ratio r/s for each horizontal acceleration

a (g)	m	n
0.05	0.046	− 0.009
0.10	0.088	− 0.018
0.15	0.116	− 0.020
0.20	0.162	− 0.029
0.25	0.201	− 0.036
0.30	0.237	− 0.042
0.35	0.273	− 0.048
0.40	0.312	− 0.055
0.45	0.338	− 0.053
0.50	0.367	− 0.055

In the third graph (Fig. 12), the horizontal axis represents the horizontal acceleration (a) as a multiple of the gravitational acceleration (g), and the vertical axis represents the angles φ_1 and φ_2 corresponding to the position of the hinges created in the collapse mechanism of a catenary arch of minimum thickness considering three different r/s ratios. When the horizontal acceleration is minimal and, consequently, the thickness of the arch is also minimal, minor variations in the obtained thrust lines result in significant variations in the angles φ_1 and

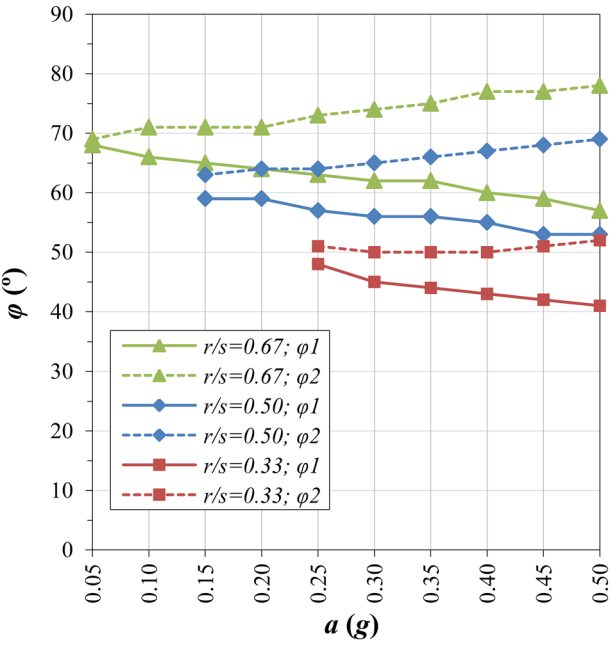

Fig. 12 Seismic acceleration and the angles φ_1 and φ_2 corresponding to the position of the hinges created in the collapse mechanism of a catenary arch of minimum thickness considering three different r/s ratios

Table 2 Parameters m and n of the equations for the straight lines which relate the horizontal acceleration to the angles φ_1 and φ_2 for each ratio r/s

r/s		m	n
0.33	φ_1	− 25.714	53.476
	φ_2	9.714	47.190
0.50	φ_1	− 17.976	61.780
	φ_2	17.738	59.923
0.67	φ_1	− 21.818	68.600
	φ_2	20.545	67.900

Table 3 Relationship between the slenderness L/ϕ of the hanging chain and the slenderness $L/t_{\min}$ of the resulting arch

r/s	$L/ø$	λ	$L/t_{\min}$
0.33	215.8	0.05	202.6
		0.10	102.8
		0.15	66.5
		0.20	50.8
		0.25	40.1
0.50	256.4	0.05	116.3
		0.10	59.0
		0.15	39.7
		0.20	29.5
		0.25	23.4
0.67	303.8	0.05	82.7
		0.10	42.6
		0.15	30.8
		0.20	22.5
		0.25	18.0

φ_2. Due to the limitations of the method, explained below, explained below, the values of the angles obtained for arches with $r/s = 0.33$ and $a < 0.25g$, and for arches with $r/s = 0.50$ and $a < 0.15g$, have been excluded from this graph. As in the two preceding graphs, the equation $\varphi_i = ma + n$ of the straight lines approximating the six curves has been defined by means of regression. Table 2 presents the parameters m and n for each straight line. It should be noted that the equations presented here are only valid for $a \in [0.05g, 0.50g]$.

Table 3 shows the relationship between the slenderness of the arch, i.e., the ratio between the length L of the catenary curve and the thickness t, and the slenderness of the hanging chain, i.e., the ratio between its length L and the spheres' diameter ø. The greater slenderness L/ϕ of the hanging chain in relation to the slenderness $L/t_{\min}$ of the resulting arch, the more accurate the result obtained by this method. According to the results showed in Fig. 2, it is possible to determine that the minimum slenderness of the hanging chain used in the physical model must be twice the slenderness of the resulting arch.

Application of the Procedure to Compound Catenary Arches

The procedure outlined in the two preceding sections can also be employed to ascertain the requisite thickness of structures made up by multiple catenary arches. To illustrate, we present an example of a structure formed by the intersection of two catenary arches. The three thrust lines can be defined by employing the chain inversion method, with consideration given to a horizontal acceleration. Subsequently, the iterative numerical process described in the preceding section can be employed to ascertain $t_{\min}$. In lieu of commencing with the equation of thrust line 1 of a known catenary, the three thrust lines were defined by means of point clouds obtained directly from the hanging chain models. This requires a slight alteration to the aforementioned calculation process. Instead of calculating the zero of the derivative of function $d_p(x)$, we directly calculate the distance from the given point of thrust line 2 to each of the points in the point cloud of thrust line 1 using Eq. (7) for all points q_i in the cloud of points making up thrust line 1, and $d_p = \min\left(d_{p,i}\right)$ the minimum of all $d_{p,i}$, according to the second way of calculation described in previous subsections. Figure 13 illustrates the application in the design of a structure formed by the intersection of two catenary arches, taking into account a horizontal acceleration of $a = 0.20g$, and includes the images of the inverted hanging chain models.

Conclusion

This paper presented a straightforward calculation method for determining the minimum thickness of a vault or catenary arch required to resist a horizontal in-plane seismic acceleration. The proposed procedure consists of two parts. In the first part, the thrust lines of the arches are defined by considering the arches' self-weight and a horizontal seismic acceleration. To achieve this, the principle of the inverted chain is employed. Here, the straight line joining the ends of the chain is tilted at an angle α from the horizontal direction, such that the tangent of α is equal to the ratio between the horizontal acceleration due to the earthquake and the acceleration of gravity. Consequently, three distinct thrust lines can be derived for a given arch. The first corresponds to the arch in a self-weight scenario, which is the catenary. The second corresponds to the arch in a self-weight scenario with the addition of a horizontal acceleration. The third is the symmetrical version of the second, accounting for the same horizontal acceleration but in an opposing direction. The second part of the procedure employed iterative numerical processes to ascertain the displacement of thrust lines 2 and 3 (which are derived from the horizontal acceleration) in relation to the catenary. Its objective was to obtain the minimum distance from these lines to the catenary. This approach is undertaken with the intention of achieving a minimal thickness for the arch inscribing the three thrust lines.

This procedure was applied to estimate the minimum thickness of three catenary arches with *r/s* ratios of 0.33, 0.50 and 0.67, taking into account ten horizontal accelerations between 0.05 g and 0.50 g. The results obtained were used to create

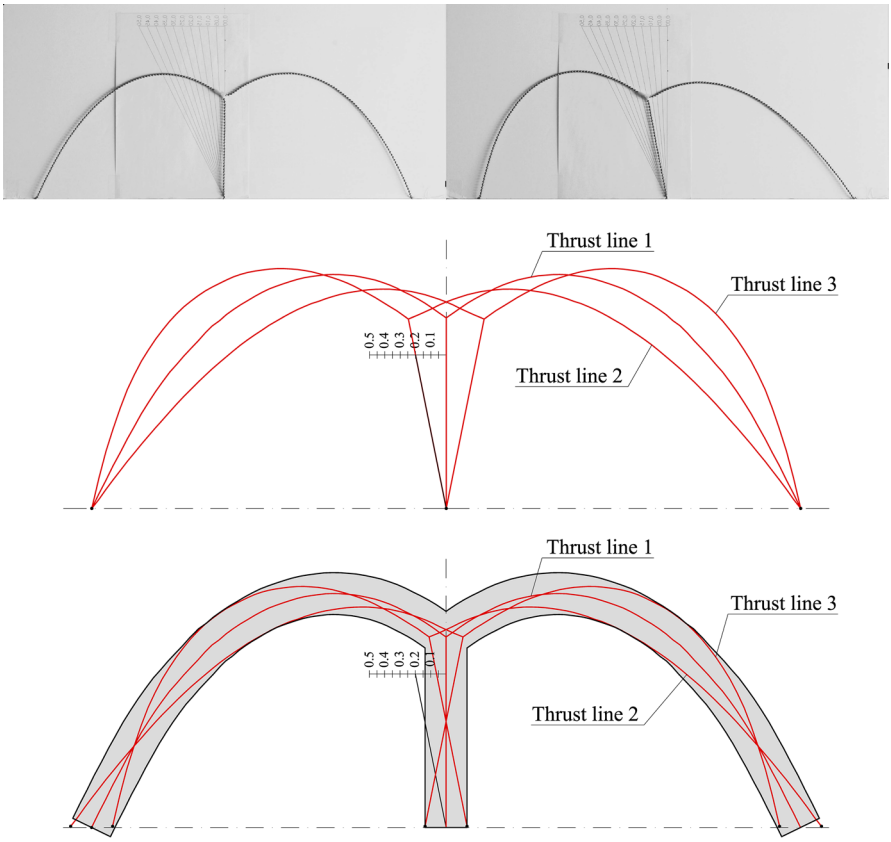

Fig. 13 Intersection of two catenary arches of minimum thickness, designed to resist a horizontal acceleration $a = 0.20g$ in both directions

three graphs. These graphs allow for the determination of two key parameters. First, the minimum requisite thickness for a given arch which has a defined *r/s* ratio and is subjected to a horizontal seismic acceleration. Second, the position of hinge formation points in the collapse mechanism of the same arch.

Moreover, the versatility of the proposed procedure has been illustrated through its application to combined arch structures. To this end, an illustrative example has been considered, comprising the intersection of two catenary arches.

It has been demonstrated that the accuracy of the outcomes yielded by this procedure, particularly regarding the angles that indicate the position of the hinges in the arch collapse mechanism, and relies upon two factors. First, the method used to measure the angle of inclination of the chain and to transform the obtained shape into a point cloud. Second, the number of points which defined each of the thrust lines.

This procedure may prove a useful tool for the preliminary design and dimensioning of constant section vault and catenary arch structures subjected to

in-plane horizontal seismic accelerations, offering a quick and straightforward approach. In any case, the design and dimensioning could subsequently be refined through the application of specific calculation processes.

Funding Open Access funding provided thanks to the CRUE-CSIC agreement with Springer Nature. Not applicable.

Data Availability Not applicable.

Code Availability All code that supports the findings of this study are available from the corresponding author upon reasonable request.

Declarations

Conflict of Interest No potential conflict of interest was reported by the authors.

References

Addis, Bill. 2014. Form finding and physical models. In *Shell structures for architecture: form finding and optimization*, eds. Sigrid Adriaenssens, Phillippe Block, Dierderik Veenendaal, and Chris Williams: 33–44. London: Routledge.

Afonso, David and Joao Fialho. 2024. Capture, optimization and transformation of physical funicular models in the digital environment: Methodological framework and application in structural design. In *Proceedings of the IASS Symposium 2024*, ed. P. Block et al.: 1–10. Zurich: IASS.

Alexakis, Haris and Nicos Makris. 2013. Minimum thickness of elliptical masonry arches. *Acta Mechanica* 224: 2977–2991. https://doi.org/10.1007/s00707-013-0906-2.

Alexakis, Haris and Nicos Makris. 2014. Limit equilibrium analysis and the minimum thickness of circular masonry arches to withstand lateral inertial loading. *Archive of Applied Mechanics* 84: 757–772. https://doi.org/10.1007/s00419-014-0831-4.

Alexakis, Haris and Nicos Makris 2023. Vector analysis and the stationary potential energy for assessing equilibrium of curved masonry structures. *Mathematics and Mechanics of Solids* 30 (1): 40-56. https://doi.org/10.1177/10812865231183335.

Bernoulli, Jacob. 1691. Solutions to the Problem of the Catenary, or Funicular Curve. *Acta Eruditorum* May: 217–219.

Block, Phillippe, Matthew DeJong and John Ochsendorf. 2006. As hangs the flexible line: Equilibrium of masonry arches. *Nexus Network Journal* 8 (2): 13–24. https://doi.org/10.1007/978-3-7643-8188-2_3.

Block, Phillippe, Matthew DeJong, Lara Davis and John Ochsendorf. 2010. Tile vaulted systems for low-cost construction in Africa. *ATDF Journal* 7 (1/2): 4-13.

Boller, Giulia, Phillippe Block and Joseph Schwartz. 2024. Heinz Isler's physical form finding of the HIB tennis shells. *Structures* 65: 106559. https://doi.org/10.1016/j.istruc.2024.106559.

Borhani, Alireza and Negar Kalanta. 2024. THINNESS: Pedagogical Form Finding Explorations in Eco-Ethical Shell Structures. In *Proceedings of the IASS Symposium 2024*, ed. P. Block et al.: 1–10. Zurich: IASS.

Bradley, Ryan, Mitchel Gohnert, Ivanka Bulovic, Adam Goliger and Daniel Surat. 2017. Steep catenary earth-brick shells as a low-cost housing solution. *Journal of Architectural Engineering* 23 (2): 04016018. https://doi.org/10.1061/(ASCE)AE.1943-5568.0000234.

Bradley, Ryan, Mitchel Gohnert and Ivanka Bulovic. 2018. Construction considerations for low-cost earth brick shells. *Journal of Construction in Developing Countries* 23 (1): 43–60. https://doi.org/10.21315/jcdc2018.23.1.3.

Cavalagli, Nicola, Vittorio Gusella and Laura Severini. 2016. Lateral loads carrying capacity and minimum thickness of circular and pointed masonry arches. *International Journal of Mechanical Sciences* 115: 645–656. https://doi.org/10.1016/j.ijmecsci.2016.07.015.

Dahmen, Joseph, and John Ochsendorfs. 2012. Earth masonry structures: arches, vaults and domes. In *Modern Earth Buildings,* eds. Matthew R. Hall, Rick Lindsay and Meror Krayenhoff, 427–460. Cambridge: Woodhead Publishing. https://doi.org/10.1533/9780857096166.4.427

DeJong, Matthew. 2009. Seismic assessment strategies for masonry structures. Doctoral dissertation, Cambridge: Massachusetts Institute of Technology.

Fallacara, Giuseppe, Ilaria Cavaliere, Johnathan Melchiorre, Giuseppe Carlo Marano and Amedeo Manuello. 2024. Reinterpretation of catenary vaulted spaces: Construction of a prototype and structural evaluation through Multibody Rope Approach. *Structures* 66: 106746. https://doi.org/10.1016/j.istruc.2024.106746.

Forgács, Tamás, Sarhosis, Vasilis and Katalin Bagi. 2017. Minimum thickness of semi-circular skewed masonry arches. *Engineering Structures* 140: 317–336. https://doi.org/10.1016/j.engstruct.2017.02.036.

Gohnert, Mitchell, and Ryan Bradley. 2020. Catenary solutions for arches and vaults. *Journal of Architectural Engineering* 26 (2): 04020006. https://doi.org/10.1061/(ASCE)AE.1943-5568.0000402.

Gohnert, Mitchel, Ivanka Bulovic and Ryan Bradley. 2018. A low-cost housing solution: earth block catenary vaults. *Structures* 15: 270-278. https://doi.org/10.1016/j.istruc.2018.07.008.

Graefe, Rainer. 2020. The catenary and the line of thrust as a means for shaping arches and vaults. In *Physical Models: Their historical and current use in civil and building engineering design*, ed. Bill Addis: 79–126. Berlin: Wilhelm Ernst & Sohn. https://doi.org/10.1002/9783433609613.ch3.

Granier, Thierry, Anders Kaye, Jerôme Ravier and Daniel Sillou. 2006. The Nubian Vault: Earth roofs in the Sahel. In *Proceedings of the conference Living in Deserts: Is a sustainable urban design still possible in Arid and hot regions* (Ghardaïa, Algeria, 9–12 December 2006): 1–14.

Gregory, David. 1697. Catenaria. *Philosophical Transactions of the Royal Society* 19 (231): 637–652.

Heyman, Jacques. 1966. The stone skeleton. *International Journal of Solids and Structures* 2 (2): 249–279. https://doi.org/10.1016/0020-7683(66)90018-7.

Heyman, Jacques. 1969. The safety of masonry arches. *International Journal of Mechanical Sciences* 11 (4): 363–385. https://doi.org/10.1016/0020-7403(69)90070-8.

Hooke, Robert. 1676. *A description of helioscopes, and some other instruments*. London.

Huerta, Santiago. 2006. Structural design in the work of Gaudi. *Architectural Science Review* 49 (4): 324–339. https://doi.org/10.3763/asre.2006.4943.

Huerta, Santiago. 2019. *El arco límite: breve historia de un problema estructural. Actas del Undécimo Congreso Nacional de Historia de la Construcción*. Instituto Juan de Herrera: Escuela Técnica Superior de Arquitectura de Madrid.

Huygens, Christiaan. 1691. The line on which it flexibly bends under its weight. *Acta Eruditorum* June: 277–291.

Johnson, Kendra, Manuela Villani, Kirsty Bayliss, Christopher Brooks, Sreyasvi Chandrasekhar, Thomas Chartier, Yen-Shin Chen, Julio Garcia-Pelaez, Robin Gee, Richard Styron, Anna Rood, Michele Simionato and Marco Pagani. 2023. Global Earthquake Model (GEM) Seismic Hazard Map. Zenodo. https://doi.org/10.5281/zenodo.8409647

Kalapodis, Nicos, Christian Málaga-Chuquitaype and Georgios Kampas. 2022. Structural efficiency of varying-thickness regolith-based lunar arches against inertial loading. *Acta Astronautica* 191: 438–450. https://doi.org/10.1016/j.actaastro.2021.11.031.

Kalapodis, Nicos, Georgios Zalachoris, Olga-Joan Ktenidou and Georgios Kampas. 2023. On the seismic behaviour of monolithic lunar arches subjected to moonquakes. *Earthquake Engineering and Structural Dynamics* 52 (1): 147–163. https://doi.org/10.1002/eqe.3754.

Kampas, Georgios, Nicos Kalapodis, Thomas McLean and Christian Málaga-Chuquitaype. 2021. Limit-state analysis of parabolic arches subjected to inertial loading in different gravitational fields using

a variational formulation. *Engineering Structures* 228: 111501. https://doi.org/10.1016/j.engstruct.2020.111501.

Leibniz, Gottfired W. 1691. The string whose curve is described as bending under its self-weight, and the remarkable resources that can be discovered from it by however many proportional means and logarithms. *Acta Eruditorum* June: 277–291.

Lengyel, Gábor. 2018. Minimum thickness of the gothic arch. *Archive of Applied Mechanics* 88: 769–788. https://doi.org/10.1007/s00419-018-1341-6.

Li, Zhi, Ting-Uei Lee, Nico Pietroni, Roland Snooks and Yi M. Xie. 2024. Design and construction of catenary-ruled surfaces. *Structures* 59: 105755. https://doi.org/10.1016/j.istruc.2023.105755.

Makris, Nicos and Haris Alexakis. 2013. The effect of stereotomy on the shape of the thrust-line and the minimum thickness of semicircular masonry arches. *Archive of Applied Mechanichs* 83: 1511–1533. https://doi.org/10.1007/s00419-013-0763-4

Málaga-Chuquitaype, Christian, Thomas McLean, Nicos Kalapodis, Christos Kolonas and Georgios Kampas. 2022. Optimal arch forms under in-plane seismic loading in different gravitational environments. *Earthquake Engineering and Structural Dynamics* 51 (6): 1522–1539. https://doi.org/10.1002/eqe.3626.

McLean, Thomas, Christian Málaga-Chuquitaype, Nicos Kalapodis and Georgios Kampas. 2021. OpenArch: An open-source package for determining the minimum-thickness of arches under seismic loads. *SoftwareX* 15: 100731. https://doi.org/10.1016/j.softx.2021.100731.

Miccoli, Stefano, Luisa María Gil-Martín and Enrique Hernández-Montes. 2023. New historical records about the construction of the Arch of Ctesiphon and their impact on the history of structural engineering. *Notes and Records* 77 (1): 113-134. https://doi.org/10.1098/rsnr.2021.0025.

Michiels, Tim and Sigrid Adriaenssens. 2018. Form-finding algorithm for masonry arches subjected to in-plane earthquake loading. *Computers and Structures* 195: 85–98. https://doi.org/10.1016/j.compstruc.2017.10.001.

Misseri, Giulia, Matthew DeJong and Luisa Rovero. 2018. Experimental and numerical investigation of the collapse of pointed masonry arches under quasi-static horizontal loading. *Engineering Structures* 173: 180–190. https://doi.org/10.1016/j.engstruct.2018.06.009.

Nikolić, Dimitrije. 2017. Thrust line analysis and the minimum thickness of pointed masonry arches. *Acta Mechanica* 228 (6): 2219-2236. https://doi.org/10.1007/s00707-017-1823-6.

Nikolić, Dimitrije. 2019. Catenary arch of finite thickness as the optimal arch shape. *Structural and Multidisciplinary Optimization* 60 (5): 1957-1966. https://doi.org/10.1007/s00158-019-02304-9.

Nikolić, Dimitrije. 2022. A note on the catenary arch bending-moment-free paradox. *Meccanica* 57 (6): 1457–1462. https://doi.org/10.1007/s11012-022-01513-9.

Nodargi, Nicola and Paolo Bisegna. 2020. Thrust line analysis revisited and applied to optimization of masonry arches. *International Journal of Mechanical Sciences* 79: 105690. https://doi.org/10.1016/j.ijmecsci.2020.105690.

Ramage, Michael, John Ochsendorf and Peter Rich. 2010. Sustainable Shells: New African vaults built with soil-cement tiles. *Journal of the International Association for Shell and Spatial Structures* 51 (4): 255-261.

Ricci, E., Aguinaldo Fraddosio, Mario D. Piccioni and Elio Sacco. 2019. A new numerical approach for determining optimal thrust curves of masonry arches. *European Journal of Mechanics-A/Solids* 75: 426–442. https://doi.org/10.1016/j.euromechsol.2019.02.003.

Sunguroglu, Defne and Guillem Baraut. 2013. Nested catenaries. *Journal of the International Association for Shell and Spatial Structures* 54 (1): 39-55.

Tempesta, Giacomo and Stefano Galassi. 2019. Safety evaluation of masonry arches. A numerical procedure based on the thrust line closest to the geometrical axis. *International Journal of Mechanical Sciences* 155: 206–221. https://doi.org/10.1016/j.ijmecsci.2019.02.036.

Ther, Ther and Lázlo P. Kollar. 2021. Dynamical similarity of multi-block catenary arches and rocking blocks subjected to horizontal base excitation. *Nonlinear Dynamics* 104 (3): 2099–2116. https://doi.org/10.1007/s11071-021-06415-1.

Vyncke, Johan, Laura Kupers and Nicolar Denies. 2018. Earth as Building Material–an overview of RILEM activities and recent Innovations in Geotechnics. *MATEC web of conferences* 149: 02001. EDP Sciences. https://doi.org/10.1051/matecconf/201814902001.

Wang, CM., and Zhang, Ji M. 2024. Maximum spanning capacity of a catenary arch under self-weight against buckling. *Australian Journal of Structural Engineering*. https://doi.org/10.1080/13287982.2024.2357403.

De Wolf, Catherine, Michael Ramage and John Ochsendorf. 2016. Low carbon vaulted masonry structures. *Journal of the International Association for Shell and Spatial Structures* 57 (4): 275–284. https://doi.org/10.20898/j.iass.2016.190.854.

Rodrigo Martín-Sáiz is an architect who obtained his Ph.D in Architecture at the Polytechnic University of Catalonia in 2015. Currently, he is an Adjunct Professor, teaching structural design at the School of Architecture of the Rovira i Virgili University. His research interests span, on one hand, the self-balancing tension structures, including tensile spoke-wheels for roofing stadiums and cable-stayed arches, and, on the other hand, the relationship between the structural behavior and the geometrical form in arches and vaults.

Blas Herrera is a geometer who obtained his Sc.D. in Mathematics at the University Autònoma of Barcelona in 1994. Presently, he is a full professor of applied mathematics –especially applied geometry– at the Rovira i Virgili University. His main fields of research interest are classical and differential geometry, and the application of geometry to architecture and engineering.